

BULLETIN OF THE CHEMICAL SOCIETY OF JAPAN VOL. 42 1795—1799 (1969)

## Role of Doped Lithium in Nickel Monoxide in the Formation of Higher Valency Nickel Oxides by Anodic Oxidation

Hiroshi YONEYAMA and Hideo TAMURA

*Department of Chemical Technology, Faculty of Engineering, Osaka University, Yamadakami, Suita, Osaka*

(Received September 27, 1968)

The anodic oxidation and cathodic reduction behavior of a sintered body of lithiated nickel oxide were studied. The electrode with the higher Li content was more active than that with the lower Li content with regard to the electrochemical oxidation and reduction in the potential range between oxygen and hydrogen evolution. The quantity of the higher-valency nickel oxide having an apparent valence state of nickel ions from  $+8/3$  to  $+4$  formed by the anodic oxidation was estimated by measuring the quantity of electricity required for reducing it to  $-0.14V$  vs. SCE. This quantity is proportional to the Li content for electrodes containing more than 0.04 atom% of Li.

Lithium ions in the electrolyte have significant effects on the charge-discharge behavior of the nickel electrode in the Ni-Cd battery system;<sup>1)</sup> for example, they increase the capacity and decrease the self-discharge. In battery systems the nickel electrode is usually prepared by "forming" nickel hydroxide, and the composition of this active mass is changed complicatedly by charge-discharge cycles.<sup>2,3)</sup> Therefore, the role of the lithium in the behavior of the electrode during charge-discharge cycles has not yet been determined quantitatively. As, however, it has been proved that lithium ion enters into the active mass by repeated charge-discharge cycles,<sup>3)</sup> the increase in the capacity of the electrode may be attributed to this phenomena. We have studied the oxidation and reduction

behavior of a nickel monoxide electrode containing a fixed amount of lithium ions in order to clarify the relation between the lithium content and the quantity of the higher valency nickel oxides formed by anodic oxidation.

### Experimental

**Chemicals.** All the chemicals used in this study were of a guaranteed reagent grade.

**Preparation of Samples.** Nickel monoxide was prepared from  $Ni(NO_3)_2 \cdot 6H_2O$  by heating it at  $600^\circ C$  for 4 hr in the air. NiO powder thus prepared contained the following impurities; Zn: 140, Ca: 330, Mg: 2750, Pb: 80, Cu: 920, Cr: 60, Mn: 190, Al, Si, Fe, trace (the contents are represented in ppm). This powder was mixed with a known amount of a  $Li_2CO_3$  solution in acetic acid. After having been mixed for about 30 min with a magnetic stirrer, they were evaporated to dryness and then heated again at  $600^\circ C$  for a few hour in the air. The powder was formed into a tablet at  $1.5 t/cm^2$  (10 mm dia. 3—5 mm thick) and this tablet was sintered at  $1200^\circ C$  for 4 hr covered with a

1) E. J. Casey, A. R. Dubois, P. E. Lake and W. J. Moroz, *J. Electrochem. Soc.*, **112**, 371 (1965).

2) G. W. Briggio and W. F. K. Wynne-Jones, *Trans. Faraday Soc.*, **52**, 1272 (1956).

3) D. Tuomi, *J. Electrochem. Soc.*, **112**, 1 (1965).

thick-layer of the same powder to prevent the Li from evaporating. After sintering, platinum contacts on the end faces of the tablet were made by firing platinum powder pasted on them at 1250°C by the procedure used in the sintering.

**Specific Resistivity of the Sample.** The specific resistivity of the sample pieces  $\rho$  was estimated from the voltage drop  $V$  between the platinum contacts, the surface area  $S$  and the thickness  $L$  of the sample, according to the  $V/I = \rho \cdot S/L$  relation, where  $I$  is the current passed through the contacts.

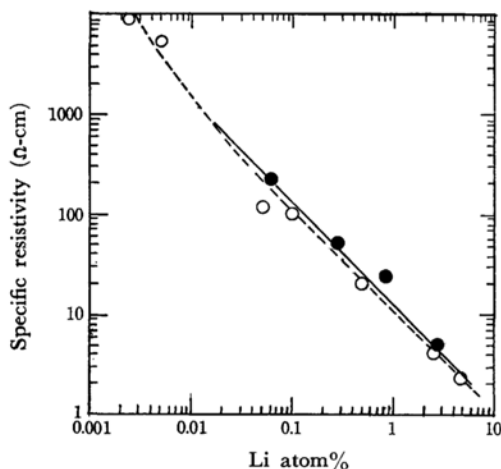


Fig. 1. Relation between Li content and resistivity at 25°C.

●— this studies, --○-- by Verway *et al.*<sup>4)</sup>

**Li Content.** The samples which were not used in the following experiments were dissolved in hot concentrated  $\text{HNO}_3$  and the Ni was removed as nickel dimethyl glyoxim. The quantity of Li in the filtrate was measured by spectrophotometry. The relations between the resistivity and Li content in the samples were very similar to the results obtained by Verway *et al.*<sup>4)</sup> as is shown in Fig. 1. From these results, the Li contents of the samples used in this study were estimated from the results of the measurement of the resistivity. The resistivities and Li contents of the test electrodes are shown in Table 1.

TABLE 1. THE SAMPLES USED AS TEST ELECTRODE

Notation of electrode	A	B	C	D	E
Resistivity at 25°C ( $\Omega\text{-cm}$ )	5.6	40	66	400	1800
Li content (atom %)	2.6	0.30	0.21	0.04	0.009

**Cell Equipment.** Before carrying out the experiment in a cell equipment, one side of the platinum contacts was erased and polished with emery papers. As these samples had a porosity of 3–10%, they were impregnated with a benzene solution of polystyrene under a vacuum and then evaporated to dryness. This

procedure was repeated a few times, and then the surface of the sample was slightly polished with 1000-mesh emery paper. The sample was then mounted in a glass tube with epoxy resin and used as the test electrode. Before the electrode behavior was examined, the resistance of this electrode was measured in 6N KOH by means of the impedance bridge and the effective electrode area was estimated, by the same procedure as was used in estimating the specific resistivity, assuming that the thickness of the sample piece used as the electrode was equal to an unmounted one. After being dipped in concentrated  $\text{HNO}_3$  and then washed with de-ionized water, the electrode was placed in a conventional cell. The cell was sealed with a rubber stopper with a gas inlet and outlet. The counter electrode was a platinized platinum plate. All the measurements were carried out at 25°C in a nitrogen atmosphere and with the light shielded. The electrolyte was 0.1N NaOH.

**Measurement of the Anodic-cathodic Behavior.** The electrode potential was measured against the SCE. In the cathodic reduction  $100 \mu\text{A}/\text{cm}^2$  was usually chosen, while in anodic oxidation various current densities, ranging from  $100 \mu\text{A}/\text{cm}^2$  to  $10 \text{mA}/\text{cm}^2$  were chosen. The oxidation-reduction cycles at each electrode did not exceed 10 in this study.

## Result

Figure 2 shows the electrode potential behavior of the A and the C electrodes when they were anodically oxidized immediately after the cathodic reduction in which their potential had attained that of hydrogen evolution. On the other hand, when they were cathodically reduced immediately after the anodic oxidation for 5 min under a fixed current density, the electrode potential was gradually changed, as is shown in Fig. 3. The phase-transition potential calculated thermodynamically is also shown in these figures (the phase transition from  $\text{Ni}_3\text{O}_4$  to  $\text{Ni}(\text{OH})_2$  or the inverse is indicated  $\text{Ni}_3\text{O}_4\text{-Ni}(\text{OH})_2$ , while another transition is also indicated in a similar fashion). As these results show, if the electrode was oxidized until its potential

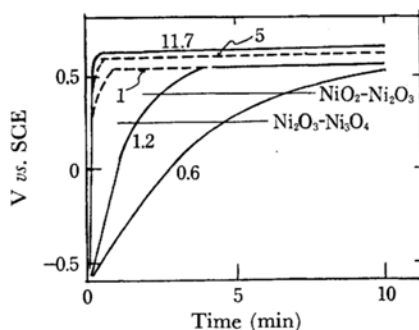


Fig. 2. Electrode potential behavior during anodic oxidation.

Solid line: 5.6  $\Omega\text{-cm}$ . Dotted line: 66  $\Omega\text{-cm}$ . The numbers in the figure represent current density ( $\text{mA}/\text{cm}^2$ ).

4) E. J. W. Verway, P. W. Haaijman, F. C. Romeijn and G. W. van Osterhout, *Philips Res. Rept.*, **5**, 173 (1950).

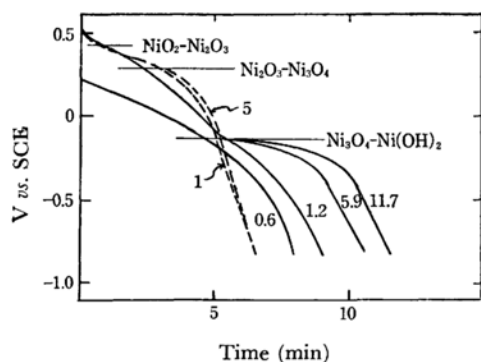


Fig. 3. Electrode potential during reduction of constant current immediately after anodic oxidation for 5 min.

Solid line: 5.6  $\Omega$ -cm, reduction current density 590  $\mu$ A/cm<sup>2</sup>. Dotted line: 66  $\Omega$ -cm, reduction current density 200  $\mu$ A/cm<sup>2</sup>. The numbers in the figure represent current density of anodic oxidation (mA/cm<sup>2</sup>).

was reached in the flat region, the behavior of the electrode potential during the cathodic reduction to  $-0.14$  V was not influenced by the current density of anodic oxidation. At the A electrode (5.6  $\Omega$ -cm), however, a stagnation of the potential change, indicating transformation from  $\text{Ni}_3\text{O}_4$  to  $\text{Ni}(\text{OH})_2$ <sup>5)</sup> was observed, and its length was influenced by the anodic-oxidation-current density. This was not observed in the C electrode (66  $\Omega$ -cm). These facts show that the nickel monoxide electrode, which contains a large amount of Li, has a tendency to undergo composition change more easily. The

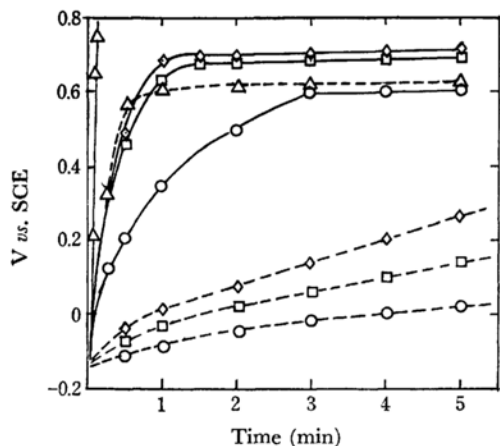


Fig. 4. Electrode potential behavior during oxidation.

Solid line: current density 1 mA/cm<sup>2</sup>. Dotted line: current density 100  $\mu$ A/cm<sup>2</sup>.

○ 5.6  $\Omega$ -cm, □ 40  $\Omega$ -cm, ◇ 400  $\Omega$ -cm, △ 1800  $\Omega$ -cm

5) The value calculated thermodynamically is  $-0.119$  V vs. SCE.

length of the stagnation of the potential change above mentioned was also influenced by the repeating cycles especially when a high current density was used in the oxidation. Therefore, in the following experiments, we studied the electrode behavior in the potential region above  $-0.14$  V.

Figure 4 shows the potential behavior of four electrode, A (5.6  $\Omega$ -cm), B (40  $\Omega$ -cm), D (400  $\Omega$ -cm), and E (1800  $\Omega$ -cm), when they were oxidized at 100  $\mu$ A/cm<sup>2</sup> and 1 mA/cm<sup>2</sup> after they had been reduced to  $-0.14$  V. The potential rise is much faster in the electrode containing less Li, and at current densities above 1 mA/cm<sup>2</sup> the electrode potential reaches the flat region within 5 min. When the electrode whose potential lay in the flat region as a result of anodic oxidation was reduced mainly at 100  $\mu$ A/cm<sup>2</sup>, the quantity of electricity  $Q$  required for reduction to  $-0.14$  V was constant for each electrode, regardless of the current density of the anodic oxidation and oxidation-reduction cycles. For example, the results obtained at the A (5.6  $\Omega$ -cm) and D (400  $\Omega$ -cm) electrodes are as shown in Table 2 while the potential

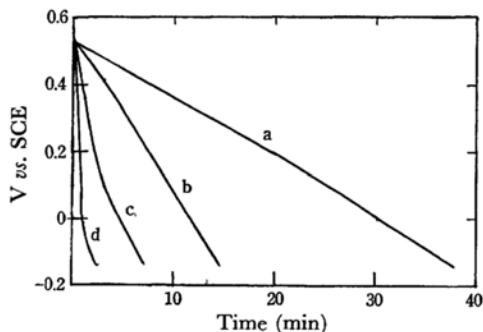


Fig. 5. Electrode potential behavior during cathodic reduction immediately after anodic oxidation. a: 5.6  $\Omega$ -cm, b: 40  $\Omega$ -cm, c: 400  $\Omega$ -cm, d: 1800  $\Omega$ -cm

TABLE 2. QUANTITY OF ELECTRICITY REQUIRED IN REDUCTION TO  $-0.14$  V OF THE OXIDES FORMED UNDER THE VARIOUS OXIDATION CONDITIONS

Electrode	Oxidation current density $\times$ time (mA/cm <sup>2</sup> ) (min)	Quantity of electricity required in reduction to $-0.14$ V (mC/cm <sup>2</sup> )
A (5.6 $\Omega$ -cm)	10 $\times$ 5	188*
	10.4 $\times$ 5	203**
	1 $\times$ 5.05	206
	1 $\times$ 10	207**
D (400 $\Omega$ -cm)	1 $\times$ 5	38.8
	0.1 $\times$ 20.9	37.5
	0.5 $\times$ 2.2	37.6
	0.5 $\times$ 5	39.3
	1 $\times$ 4.8	38.7

Reduction current density was 100  $\mu$ A/cm<sup>2</sup>, except for \* 50  $\mu$ A/cm<sup>2</sup>, \*\* 1 mA/cm<sup>2</sup>.

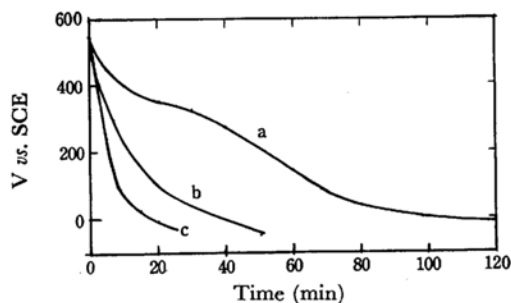


Fig. 6. Behavior of open circuit potential after oxidation up to oxygen evolution under the oxidation condition ( $\text{mA}/\text{cm}^2 \times \text{min}$ ).

a:  $5.6 \Omega\text{-cm}$  ( $1 \times 16$ ), b:  $40 \Omega\text{-cm}$  ( $0.1 \times 23$ )  
c:  $400 \Omega\text{-cm}$  ( $1 \times 3$ )

behavior of each electrode during reduction to  $-0.14 \text{ V}$  is as shown in Fig. 5. When the electrodes were open-circuited after oxidation up to the oxygen evolution, the potentials of these electrode gradually fell, as Fig. 6 shows. On the other hand, when the electrodes were reduced to  $-0.14 \text{ V}$  at  $100 \mu\text{A}/\text{cm}^2$ , a build-up of the potential was observed after the reduction current had been interrupted at various potentials between that of oxygen evolution and  $-0.14 \text{ V}$ , though at the A electrode it did not appear clearly. Even with this electrode, however, this phenomenon was observed distinctly when the reduction-current density was  $10 \text{ mA}/\text{cm}^2$ . When the reduction current was interrupted at a potential below  $-0.14 \text{ V}$ , the build-up of potential was observed distinctly and the potential of the electrode easily reached  $-0.14 \text{ V}$  or more, as is shown in Fig. 7.

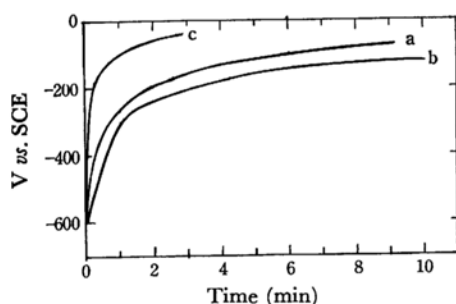


Fig. 7. Behavior of electrode potential after reduction down to  $-0.6 \text{ V vs. SCE}$  under the reduction current density ( $\text{mA}/\text{cm}^2$ ).

a:  $5.6 \Omega\text{-cm}$  ( $1 \text{ mA}/\text{cm}^2$ ), b:  $40 \Omega\text{-cm}$  ( $0.1 \text{ mA}/\text{cm}^2$ ), c:  $400 \Omega\text{-cm}$  ( $0.1 \text{ mA}/\text{cm}^2$ )

### Discussion

The quantity of electricity  $Q$  obtained by reducing the electrode to  $-0.14 \text{ V}$  is calculated to be  $10\text{--}200 \text{ mC}/\text{cm}^2$ , depending on the Li content in the electrode.  $Q$  is nearly equivalent to the quantity

of the higher-valency nickel oxides, with the apparent valence state of nickel ions ranging from  $+8/3$  to  $+4$ .

Taking the specific gravity of NiO as 6.66, the number of Ni ions per sq. cm of the NiO electrode surface is calculated to be  $1.4 \times 10^{15}/\text{cm}^2$ . Although the specific gravity may be changed by doping the Li, it could not be changed greatly in this study because the electrode in this study contained only 2.6 atom% Li at most. Therefore, if it is supposed that  $1.4 \times 10^{15}/\text{cm}^2$  divalent nickel ions exist on the electrode surface and that all of these ions are oxidized to the tetravalent,  $Q$  is calculated to be  $0.3 \text{ mC}/\text{cm}^2$ . By comparing this calculated  $Q$  value with the experimental  $Q$  value, the nickel ions participating in the electrochemical reaction amount to  $30\text{--}600$  times the value calculated, depending on the Li content. This suggests the depth of the NiO ion layer from the surface participating in the reaction at potentials above  $-0.14 \text{ V}$ . However, by considering the error introduced in the estimation of the specific resistivity, the true electrode area must be much larger than the apparent area, hence, the reaction is limited in the thinner surface layer of the electrode.

When NiO is oxidized electrochemically, oxygen ions enter into the NiO lattice. As the NiO electrode was confirmed to be well crystallized by X-ray diffraction, the transfer of oxygen ions into the interior of the NiO crystal may be difficult. Considering the fact that  $Q$  is constant regardless of the oxidation conditions, the formation of higher-valency oxides with apparent valence states from  $+8/3$  to  $+4$  is limited by some factor related to the crystal structure rather than with the rate of the diffusion of oxygen ions. This is also suggested by the results shown in Fig. 3. In this figure the plateau showing a transition from  $\text{Ni}_3\text{O}_4$  to  $\text{Ni}(\text{OH})_2$  appears at the A electrode in proportion to the current density of anodic oxidation, though the potential behavior is coincident at higher potentials. This phenomenon may indicate that oxygen ions are transferred into the NiO lattice in proportion to the electric field across the electrode in such a way that one oxygen ion is arranged into three ion pairs of  $\text{Ni}^{2+}$  and  $\text{O}^{2-}$  after the formation of the higher-valency oxides with apparent valence states of nickel ions from  $+8/3$  to  $+4$ . Probably this structure would be energetically most stable.

Nickel hydrate is probably formed at potentials above  $-0.14 \text{ V}$ , and  $\text{Ni}(\text{OH})_2$  is formed below this potential while reducing the electrode. The former can not be produced in a quantity more than the equivalent of  $Q$ , the formation of the latter is also considered to be poor, for the potential of the electrode easily fell to that of the hydrogen evolution and the recovery of the electrode potential after interrupting the reduction current at potentials lower than  $-0.14 \text{ V}$  was quick as is shown in

Fig. 7. The difficulty of the formation of  $\text{Ni}(\text{OH})_2$  may be due to the same reason as in the formation of the higher-valency oxides; that is, in this case the transfer of  $\text{H}_2\text{O}$  into the  $\text{NiO}$  lattice is apparently necessary to convert  $\text{NiO}$  to  $\text{Ni}(\text{OH})_2$ , and this is probably difficult. Therefore, it is probable that  $\text{Ni}_3\text{O}_4$  was reduced to  $\text{NiO}$  on the plateau of the potential showing the conversion of  $\text{Ni}_3\text{O}_4$  to  $\text{Ni}(\text{OH})_2$  in Fig. 3.<sup>6)</sup>

On the basis of the finding that  $Q$  was constant on each electrode, almost all of the protons in nickel hydrate or  $\text{Ni}(\text{OH})_2$  were considered to be possibly transferred into the electrolyte when the electrode was oxidized under the experimental

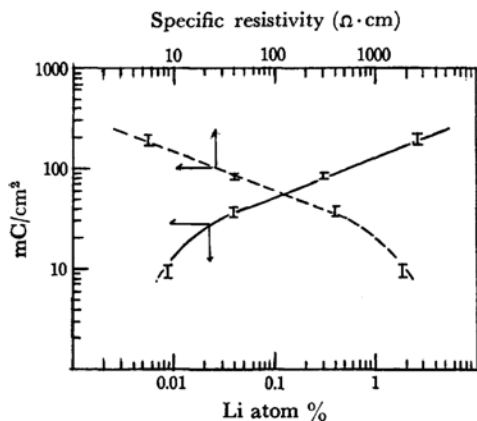


Fig. 8. Plot of  $Q$  against Li content and resistivity of the electrode.

6) The potential of the transition from  $\text{Ni}_3\text{O}_4$  to  $\text{NiO}$  is  $-0.142$  V vs. SCE.

conditions. This is probable because the hydrate or hydroxide layer was very thin, if it was present at all.

The  $Q$  values at each electrode are plotted against the resistivity of the electrode and the Li content in Fig. 8. In the case of Li contents more than 0.04 atom%, the following relationship exists between  $Q$  and the Li content  $C$  in  $\text{NiO}$ , if allowance is made for the accuracy of  $Q$  being within  $\pm 5\%$ .

$$\log Q = 0.40 \log C + 2.14$$

where  $Q$  is shown in  $\text{mC}/\text{cm}^2$  and  $C$ , in atom%.

In the reduction period, diffusion of ions in the electrode-surface region is slow, especially at low Li contents, hence,  $Q$  does not indicate correctly the quantity of the higher-valency oxides with the apparent valence states of nickel ions from  $+8/3$  to  $+4$ , especially at electrodes of low Li contents. In order to make  $Q$  exactly equivalent to the quantity of the higher valency oxides in question, the lower current density must be adopted, but if this is done the error based on self-discharge, shown in Fig. 6 will be introduced. The departure of  $Q$  at the E electrode from the above relation may be related to the error introduced by the slowness of the diffusion of ions.<sup>7)</sup>

When Li is doped in  $\text{NiO}$ , the divalent nickel ions equal to the amount of doped Li are converted to the trivalent state. Therefore, whether  $Q$  is large or small supposedly depends on the amount of trivalent nickel ions in monoxide.

7) S. Yoshizawa, Z. Takehara, M. Kato and K. Kumazaki, *Denki Kagaku (J. Electrochem. Soc. Japan)*, **34**, 661 (1966).